Conf-770412--1

SAND-77-0281C

HYDRODYNAMIC INSTABILITIES IN INERTIAL CONFINEMENT FUSION*

J. R. Freeman
Sandia Laboratories
Albuquerque, New Mexico 87115

Text for invited talk to be presented at
1977 Washington Meeting of the American Physical Society,
April 25-28, 1977

ABSTRACT

Inertial confinement fusion targets generally consist of hollow high-density spheres filled with low density thermonuclear fuel. Targets driven ablatively by electrons, ions, or lasers are potentially unstable during the initial acceleration phase. Later in time, the relatively low density fuel decelerates the dense inner portion of the sphere (termed the pusher), permitting unstable growth at the fuel-pusher interface. The instabilities are of the Rayleigh-Taylor variety, modified by thermal and viscous diffusion and convection. These problems have been analyzed by many in recent years using both linearized perturbation methods and direct numerical simulation. Examples of two-dimensional simulations of the fuel-pusher instability in electron beam fusion targets will be presented, along with a review of possible stabilization mechanisms.

---

*This work supported by the U. S. Energy Research and Development Administration.

I. Introduction

Inertial confinement fusion is based on using lasers, electron, or ion beams to compress and heat targets which either consist of or contain deuterium and tritium fuel. A typical target for electron beam fusion is shown in the first slide. The electron beam energy is deposited in an outer layer, termed the ablator. This increases its pressure, causing the outer portions to expand or ablate outward. To conserve momentum, the inner portion, termed the pusher, is driven inwards towards the center, compressing and heating the fuel. Since the ablation products are of a lower density than the pusher, this process is hydrodynamically unstable. Although similar to the classic Rayleigh-Taylor instability, the behavior in this case is modified by finite density and pressure gradients, thermal and viscous diffusion, and strong convection through the region of instability. In particular, these targets are unstable in a relatively narrow spatial region bounded by the peaks of the density and pressure profiles.

Considerable theoretical work has been done for instabilities in the ablator-pusher region. A linearized spherical harmonic numerical treatment has been developed by workers at LASL and Rochester, while analytic studies have been performed by Kidder of LLL and Brueckner of UCSD. An alternative approach has used direct computer simulation of the instabilities using two-dimensional hydrodynamics codes. This work has been pursued by groups at LLL, Sandia, LASL, and by Jay Boris at NRL. Work reported at the Electron Beam Conference held somewhat over a year ago at Sandia indicated that the broad deposition profile of electrons led to greater stability over targets driven by ions or lasers.

I would like today to concentrate on two types of instabilities of the fuel-pusher interface which can occur later in time, when shock waves and the compressed fuel begin to decelerate the pusher. These instabilities are of interest because they can arise in targets driven by any power source and can even arise in uniformly heated targets which are perfectly stable at their outer surface. The next slide shows a radius vs. time plot for a thin uniformly heated iron target designed for present day e-beam machines by Milt Clauser.[1] A shock wave is produced in the fuel by the acceleration process; this wave traverses the fuel, ultimately reflecting at the origin and returning to the fuel-pusher interface. The passage of the shock through the interface causes it to decelerate momentarily. This change in velocity results in an instability which allows spatial perturbations to grow. The shock wave divides into a transmitted and a reflected shock, the latter of which can travel inwards and repeat the process. As fuel is heated and compressed by the shocks and the pusher, the pressure increases to the point at which the fuel pressure exceeds the pusher pressure. The pressure gradients act to decelerate the pusher, thereby subjecting the fuel-pusher interface to Rayleigh-Taylor instabilities. The initial amplitudes of perturbations for this stage of the instability are quite probably determined by the earlier shock induced perturbation growth.

We have used two-dimensional numerical simulations to study these phenomena. I will first describe work in which the perturbation growth is dominated by the fuel-pressure-induced deceleration of the pusher and then present results from a separate study of the shock-induced instability.

II. Fuel Pressure Gradient Induced Instabilities

One object of our study has been to test the validity of what has become known as the free-fall time. This simple model assumes that the shortest wavelengths of the Rayleigh-Taylor grow up rapidly and form spikes which coast in at about the maximum pusher velocity. The trajectory of these spikes is shown as the free-fall line on the slide. The effect of the spikes on the output of the target is then approximated in 1-D calculations by ending the calculation at the time the spikes free-fall to the origin. Any output occurring after this time would presumably be lost.

We have constructed a 2-D planar model for the particular spherical target described. A planar model omits the convergence effects but enhances the separation between the free-fall time and the turnaround or implosion time. There is no compelling reason to perform 2-D computations of the entire implosion. We have thus used a conventional 1-D code to compute the behavior until the initial time of deceleration. The configuration at that time is then used as initial conditions for a 2-D computation with a surface or velocity perturbation added to the interface. We have used a 2-D hydrodynamics code entitled CSQ,[2] written by Sam Thompson of Sandia. The code is basically Eulerian but uses Lagrangian finite difference methods to preserve interfaces.

The next slide shows the r-t plot arising from the 1-D unperturbed case, and also plots the average fuel temperature vs. time. The enhanced separation brought on by the planar model is evident. We chose a perturbation wavelength of 10 μ, about equal to the final fuel dimensions and have initiated the runs with either a .05% velocity perturbation or a 1% surface perturbation. The next slide shows the configuration just after the initiation of the perturbation. The iron region is above, the D_2 region is below. Sixteen zones per wavelength were used for numerical resolution. The next series of slides shows the reflected and transmitted shocks, as well as the non-linear growth of the spikes.

The next slide shows again the r-t plot from the time of deceleration and plots the trajectory of the central spike. One observes that the spikes take an appreciable amount of time to grow and saturate to a free-fall velocity. This then would permit a greater time for fuel-output before the spikes arrived at the origin. The next slide shows the implications of this by plotting the neutron output vs. time from the original 1-D spherical run. One sees that a slight relaxation of the free-fall restriction can make the difference in whether neutrons would be detected. The major concern remaining relates to the behavior of faster growing, shorter wavelengths spikes.

III. Shock-Induced Interface Instability

As indicated earlier, the fuel-pusher interface is unstable to shock passage even in the absence of any other motion or acceleration of the interface. This problem was first studied by R. D. Richtmyer,[3] who presented results, shown on the next slide, from a linear theory for both incompressible and compressible flow. An experiment was later performed with helium and air by Meshkov[4] which verified the basic behavior but resulted in much lower growth rates than the linear theory. The Meshkov experiments were done with very large initial amplitudes which were well into the non-linear regime, so that this lack of comparison is possibly not surprising. A few years later Meyer and Blewett[5] of LASL used a 2-D Lagrangian code to study the Meshkov experiments. They obtained qualitative agreement, but found growth rates closer to the linear results. Because of mesh tangling difficulties, these results were limited to relatively small amplitudes.

We have used the CSQ code to study the shock interface stability problem for the iron target already described. The Eulerian features of the code permit the calculations to extend to much larger amplitudes than before. Simple shock wave theory predicts that after the shock passage, the interface becomes a contact discontinuity moving at a constant velocity. We have elected to perform our computations in a frame moving with the post-shock contact surface velocity, thereby providing a way for keeping the interface growth within the computational mesh.

The next series of slides shows the growth of a 1 μ wavelength perturbation which was initiated with a .1 μ surface perturbation. The growth is due solely to the shock wave passage. As a check on the code and method of computation, we computed a 10 μ case initiated by a .1 μ initial amplitude. The results, shown on the next slide, agree with linear theory to about 15%. This agreement is obtained by using the initial perturbation just after the shock passage on the linear formula, as noted by Meyer and Blewett. If we make a similar plot for the 1 μ sequence, we see that the growth at large amplitudes is much lower than the linear prediction. A simplified analytic model developed by Lou Baker of Sandia is shown for comparison. From these results we conclude that shock-induced instabilities must be considered in any stability analysis of a particular design, but note that the non-linear growth is much slower than the linear approximation.

IV. Conclusions

To summarize (next slide), we feel that inner surface instabilities are an important concern for all ICF targets. The results to date indicate that wavelengths on the order of final fuel dimensions are less of a problem than the shorter wavelengths. The last slide describes possible remedies presently on study. The simplest, of course, is to obtain the output before instabilities grow. This can often be done by doubling the input power driving the target. Bangerter and Meeker[6] of LLL reported on an interesting design for an ion beam target which uses an inner shell whose compressed density equals the fuel density. Viscous and thermal stabilization become important at very short wavelengths, but do not appear helpful in the regime that we've studied. A recent paper by Menikoff,[7] et al. from LASL suggests that simple mass diffusion may play an important role in reducing the density gradients of the interface. Finally, various Soviet workers, including Afanasev,[8] have alluded to turbulent mixing as a mechanism for stabilization.

References

1. M. J. Clauser, "Thin Shell Targets for Neutron-Producing Implosions with Low-Power Electron Beams," Sandia Laboratories Report, SAND-76-0158 (March 1976).
2. S. L. Thompson, "CSQ - A Two-Dimensional Hydrodynamics Program with Energy Flow and Material Strength," Sandia Laboratories Report, SAND-74-0122 (August 1975).
3. R. D. Richtmyer, Comm. on Pure and Appl. Math. 13, 297 (1960).
4. Ye. Ye. Meshkov, NASA Tech. Trans. No. NASA-Tt F-13, 074, 1970 (unpublished).
5. K. A. Meyer and P. J. Blewett, Phys. Fluids 15, 753 (1972).
6. R. Bangerter and D. Meeker, "Ion Beam Inertial Fusion Target Designs," Preprint UCRL-78474, (October 1976).
7. R. Menikoff, R. C. Mjolsness, D. H. Sharp, and B. J. Doyle, to be published in Physics of Fluids.
8. Yu. F. Afanasev, N. G. Basov, E. G. Gamalii, O. N. Krokhin, and V. B. Rozanov, JETP Lett. 23, 567 (1976).

FIGURE 1

ELECTRON BEAM FUSION TARGET

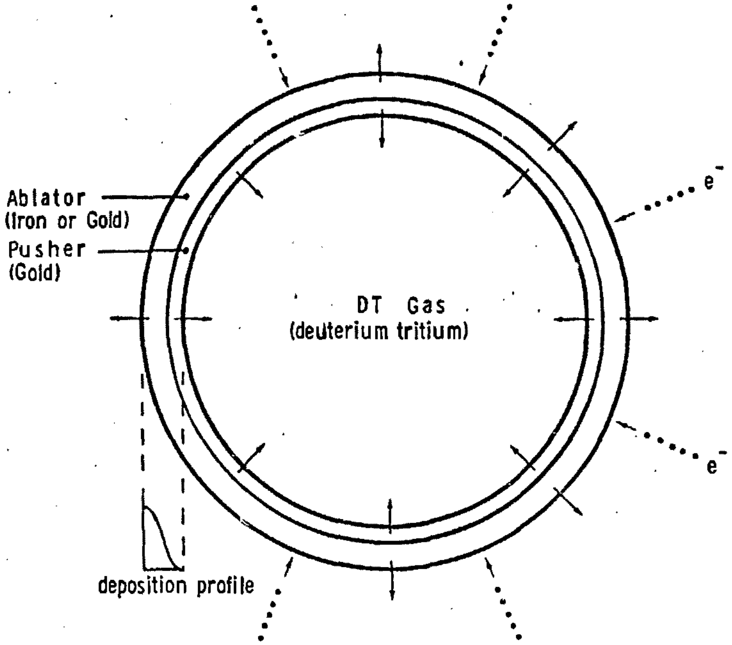

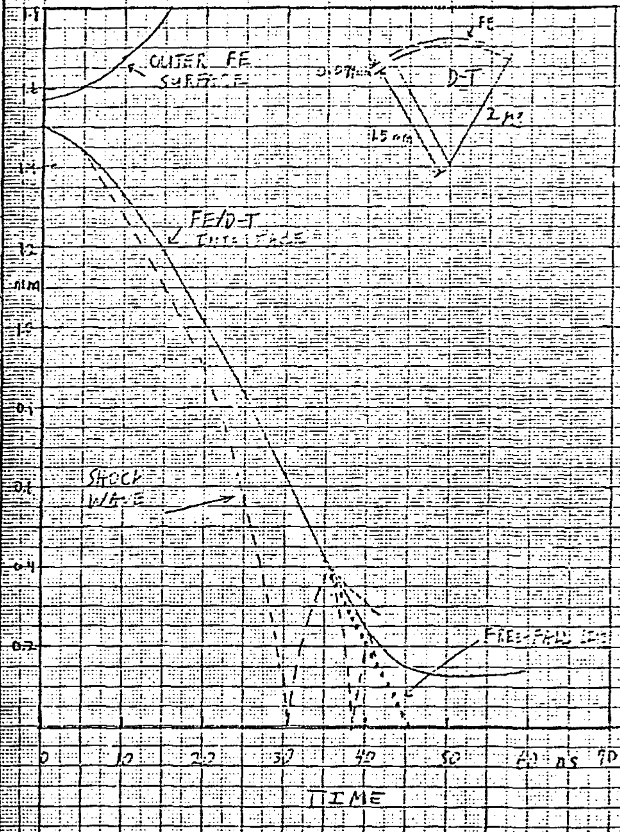
OUTER FE SURFACE
FE
0.07 mm
D-T
2 mm
.15 mm
FE/D-T INTERFACE
SHOCK WAVE
FREE-FALL LINE
RADIUS
mm
1.8
1.6
1.4
1.2
1.0
0.8
0.6
0.4
0.2
0
10
20
30
40
50
60
ns
70
TIME

FIGURE 2

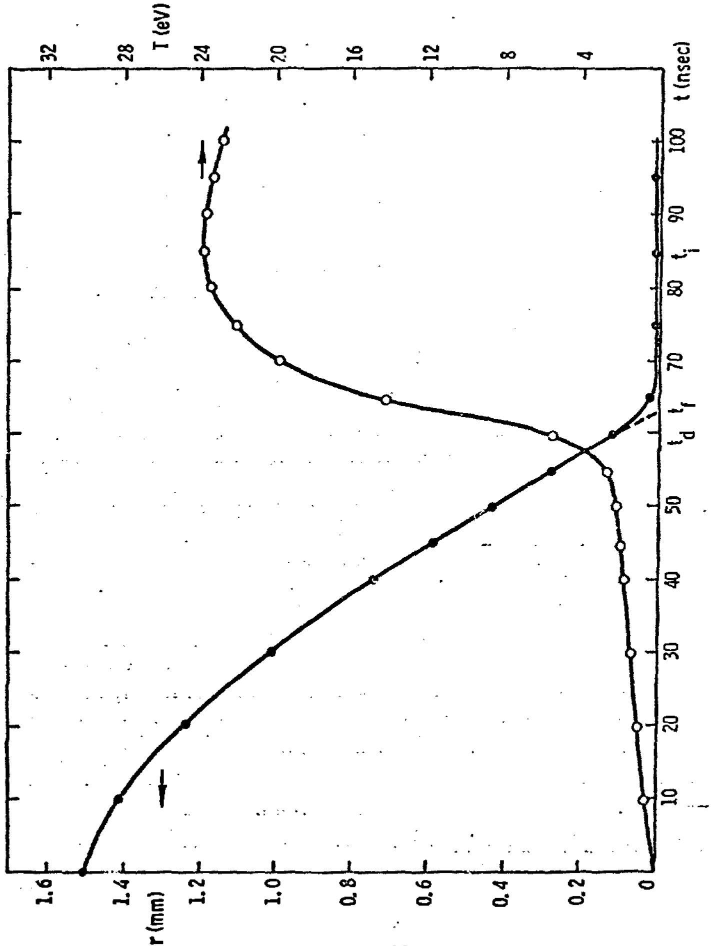
T (eV)
32
28
24
20
16
12
8
4
t (nsec)
10
20
30
40
50
t_d
t_f
70
80
t_i
90
100
r (mm)
1.6
1.4
1.2
1.0
0.8
0.6
0.4
0.2
0

FIGURE 3

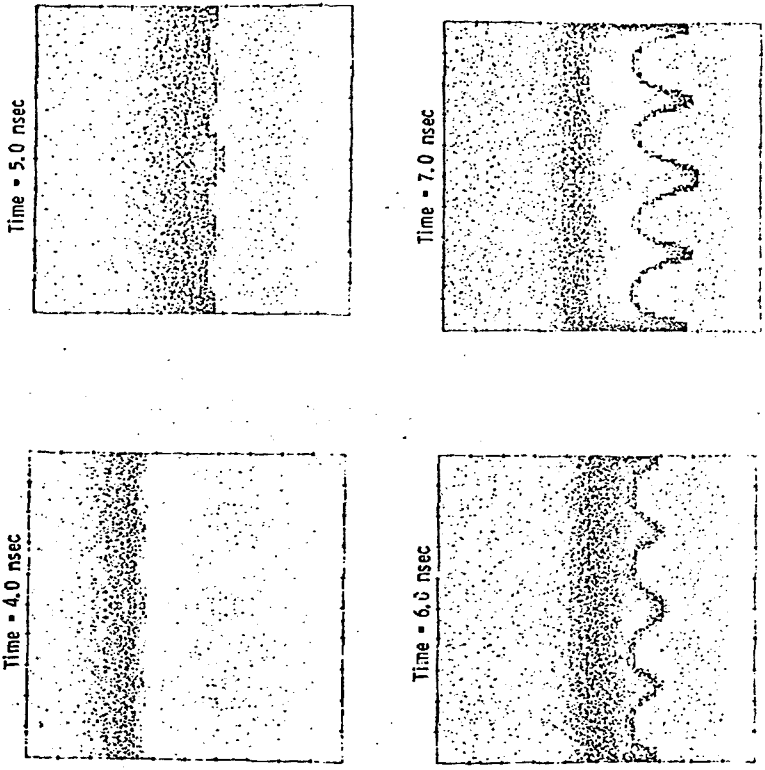

FIGURE 4a

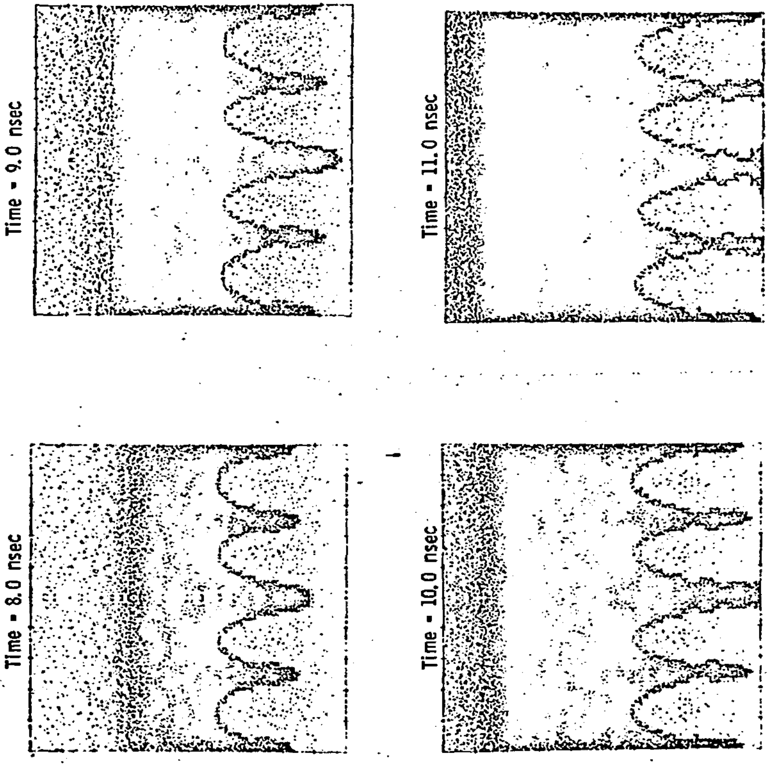

FIGURE 4b

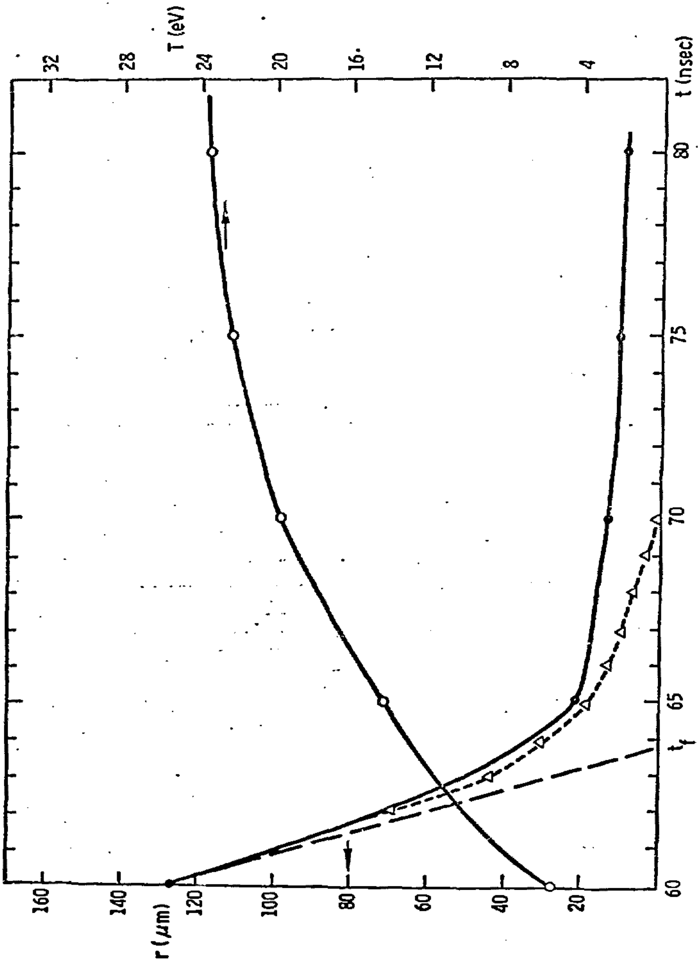
r (μm)
20
40
60
80
100
120
140
160
T (eV)
4
8
12
16
20
24
28
32
t (nsec)
60
65
70
75
80
t_f

FIGURE 5

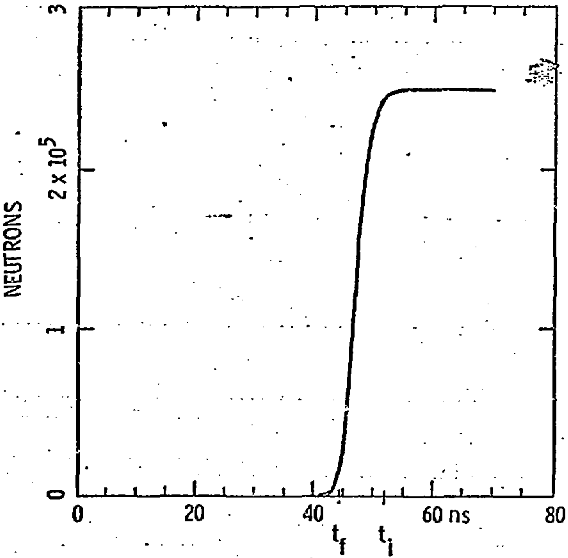

FIGURE 6

FIGURE 7

LINEAR THEORY OF SHOCK INDUCED INSTABILITY

(R. D. Richtmyer, Comm. on Pure and Appl. Math. 13, 297 (1960)

$$Z_0 = \eta_0 \cos kx \quad , \quad k\eta << 1$$

$$\frac{d^2\eta}{dt^2} = k\, g\, \eta (\rho_+ - \rho_-)/(\rho_+ + \rho_-)$$

$$\frac{d\eta}{dt} = k\, v_c\, \eta_0 (\rho_+ - \rho_-)/(\rho_+ + \rho_-) \equiv \eta_0 \gamma$$

$$\eta = \eta_0 (1 + \gamma t)$$

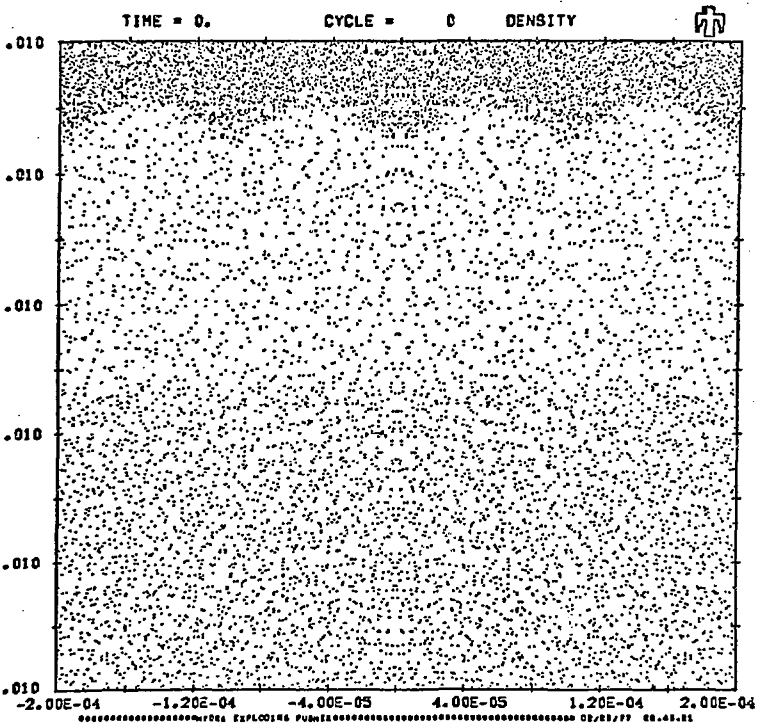
TIME = 0.
CYCLE = 0
DENSITY
.010
.010
.010
.010
.010
.010
-2.00E-04
-1.20E-04
-4.00E-05
4.00E-05
1.20E-04
2.00E-04

FIGURE 8a

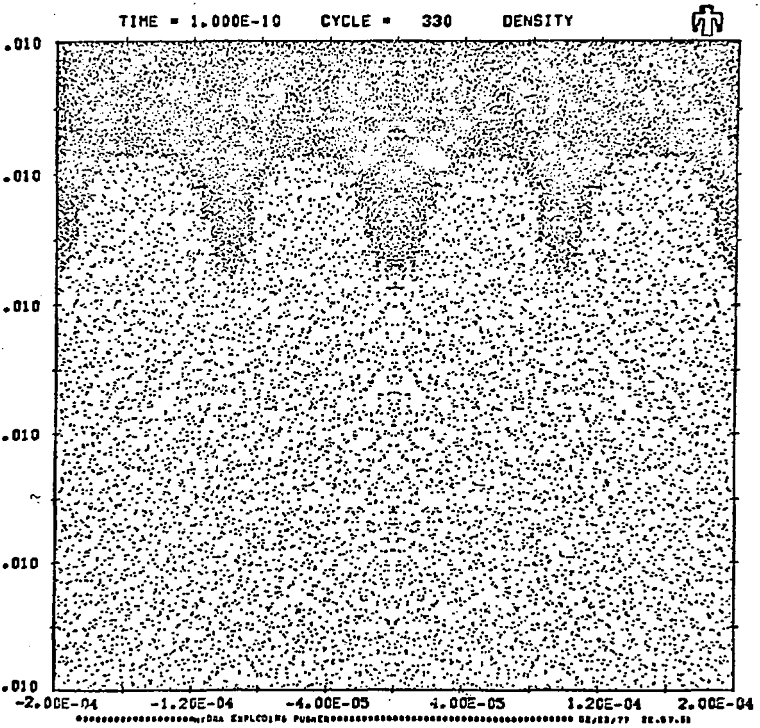
TIME = 1.000E-10
CYCLE = 330
DENSITY
.010
.010
.010
.010
.010
.010
-2.00E-04
-1.20E-04
-4.00E-05
4.00E-05
1.20E-04
2.00E-04

FIGURE 8b

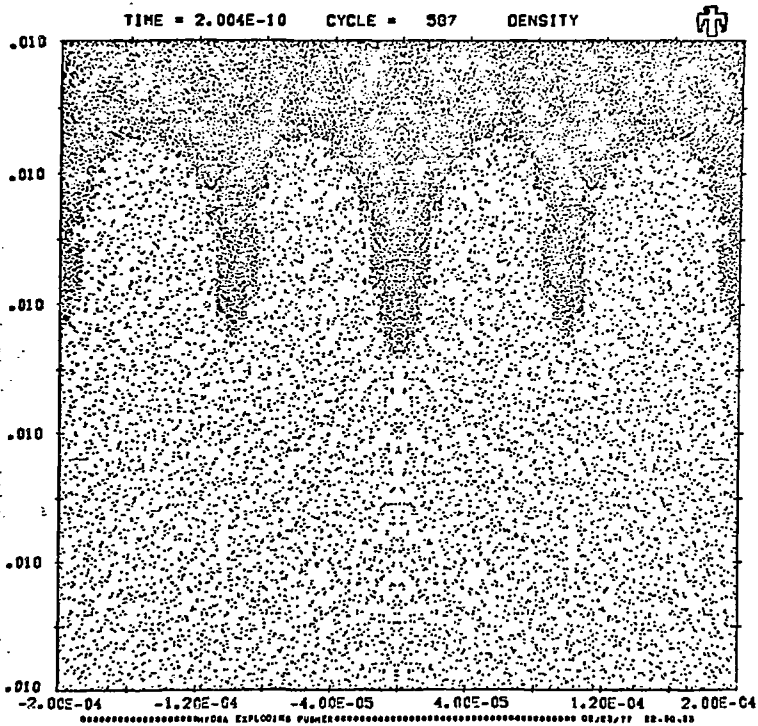
TIME = 2.004E-10
CYCLE = 587
DENSITY
.010
.010
.010
.010
.010
.010
-2.00E-04
-1.20E-04
-4.00E-05
4.00E-05
1.20E-04
2.00E-04
EXPLODING PUSHER

FIGURE 8c

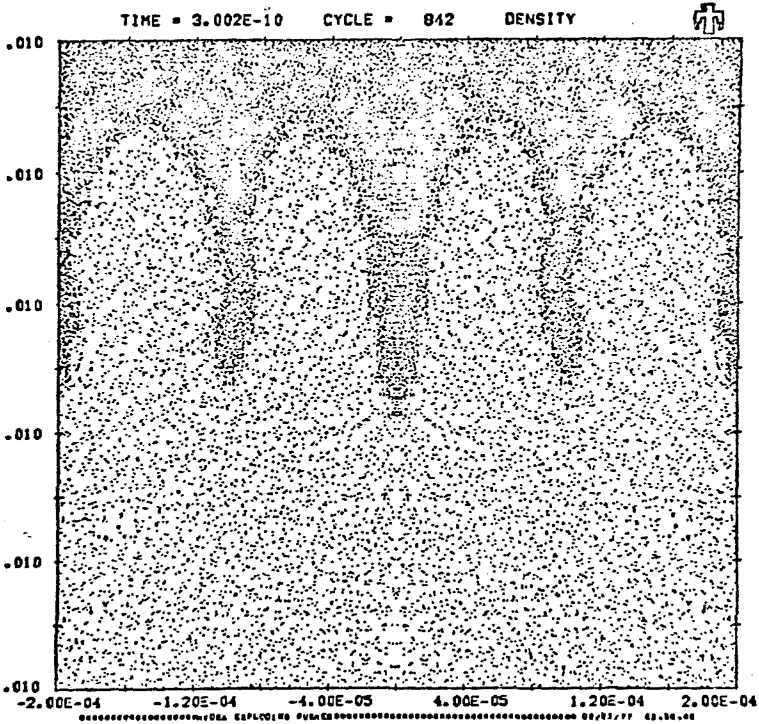
TIME = 3.002E-10 CYCLE = 842 DENSITY
.010
.010
.010
.010
.010
.010
-2.00E-04
-1.20E-04
-4.00E-05
4.00E-05
1.20E-04
2.00E-04

FIGURE 8d

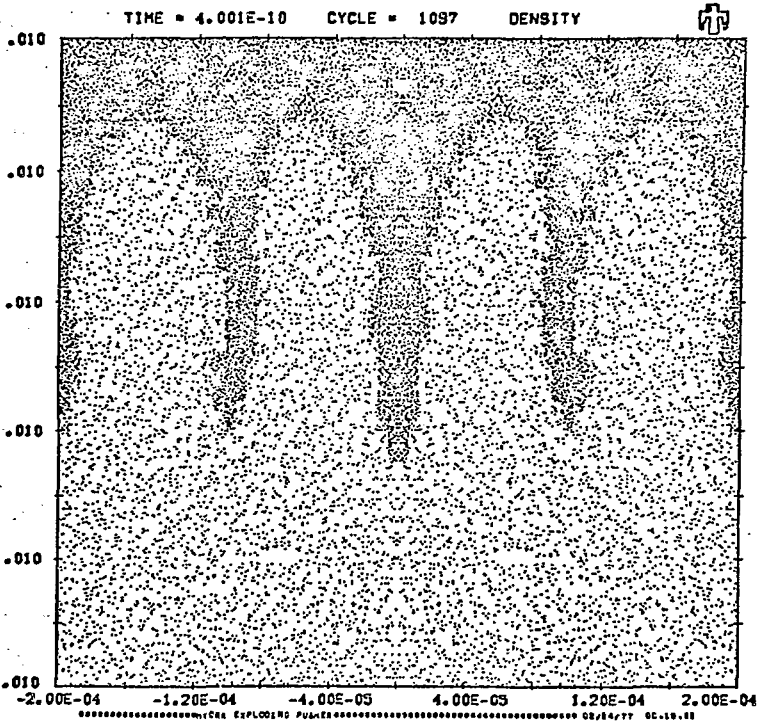
TIME = 4.001E-10
CYCLE = 1097
DENSITY
.010
.010
.010
.010
.010
.010
-2.00E-04
-1.20E-04
-4.00E-05
4.00E-05
1.20E-04
2.00E-04
EXPLODING PUSHER

FIGURE 8e

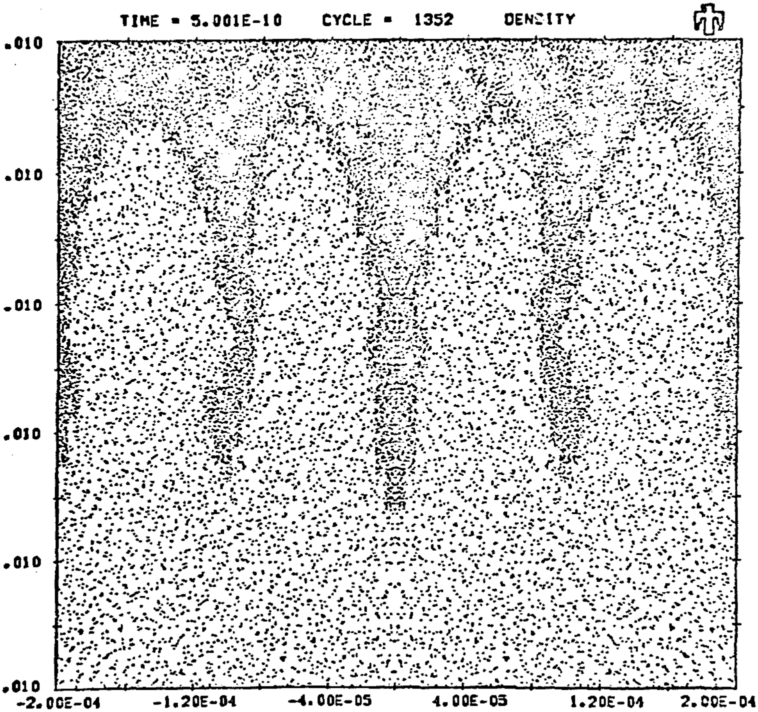
TIME = 5.001E-10 CYCLE = 1352 DENSITY
.010
.010
.010
.010
.010
.010
-2.00E-04
-1.20E-04
-4.00E-05
4.00E-05
1.20E-04
2.00E-04

FIGURE 8f

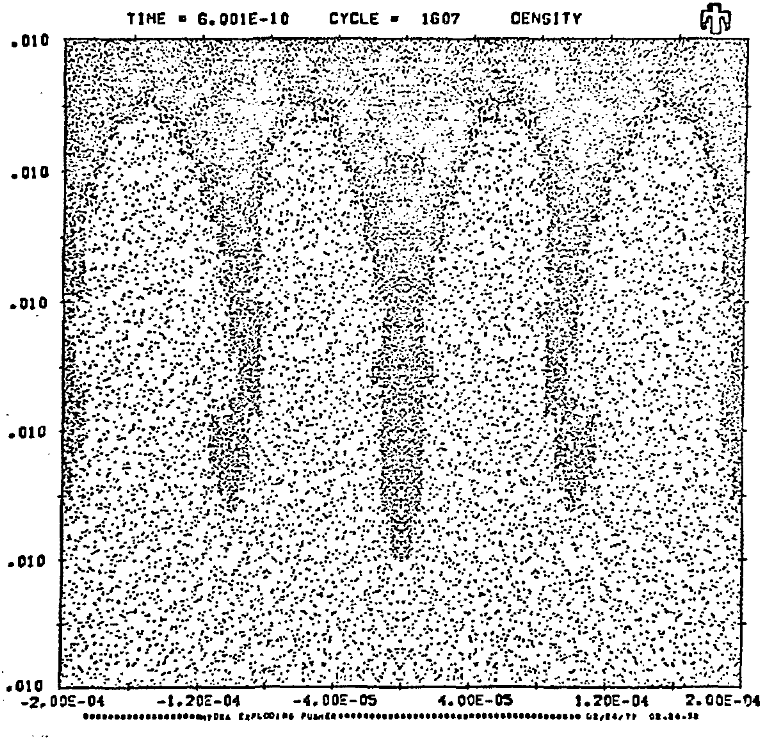
TIME = 6.001E-10
CYCLE = 1607
DENSITY
.010
.010
.010
.010
.010
.010
-2.00E-04
-1.20E-04
-4.00E-05
4.00E-05
1.20E-04
2.00E-04
HYDRA EXPLODING PUSHER

FIGURE 8g

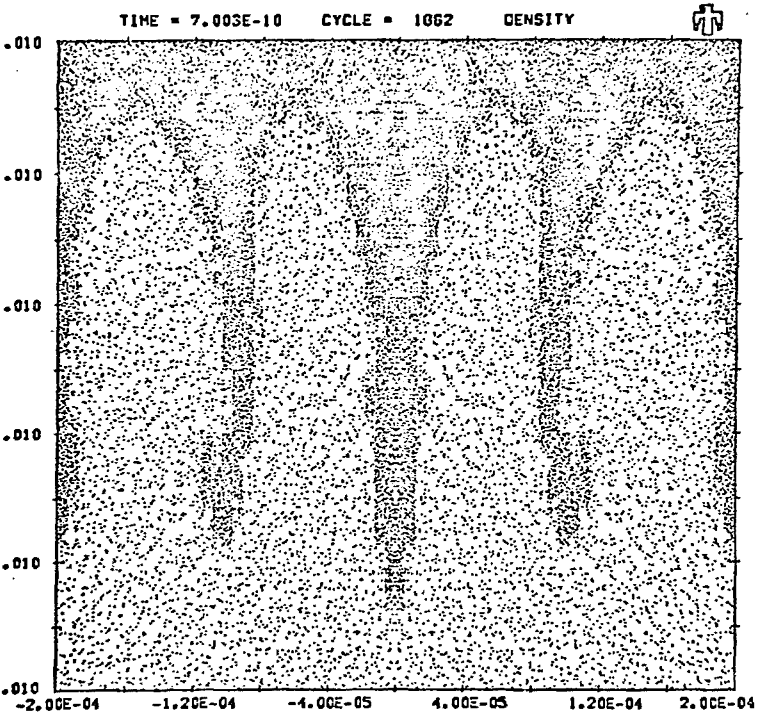
TIME = 7.003E-10
CYCLE = 1062
DENSITY
.010
.010
.010
.010
.010
.010
-2.00E-04
-1.20E-04
-4.00E-05
4.00E-05
1.20E-04
2.00E-04

FIGURE 8b

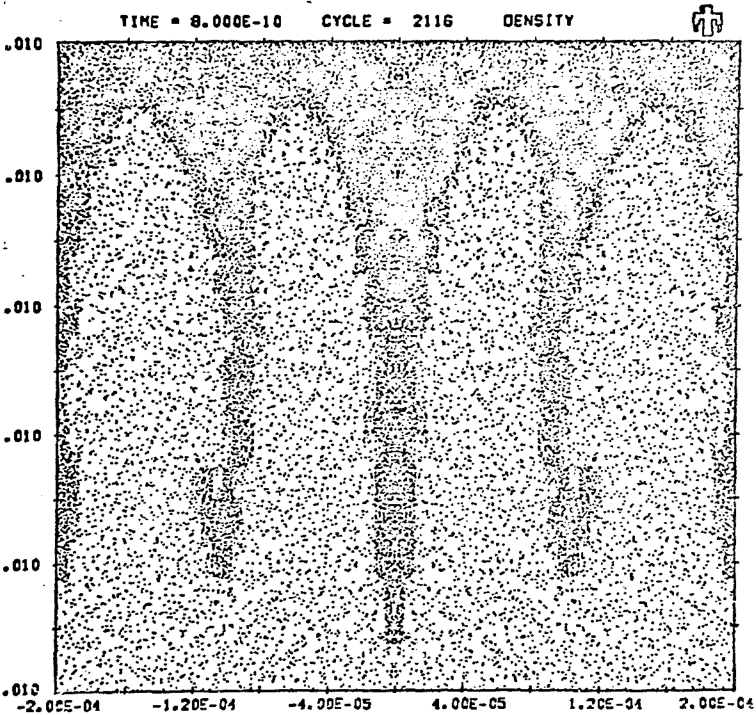
TIME = 8.000E-10
CYCLE = 2116
DENSITY
.010
.010
.010
.010
.010
.010
-2.00E-04
-1.20E-04
-4.00E-05
4.00E-05
1.20E-04
2.00E-04

FIGURE 81

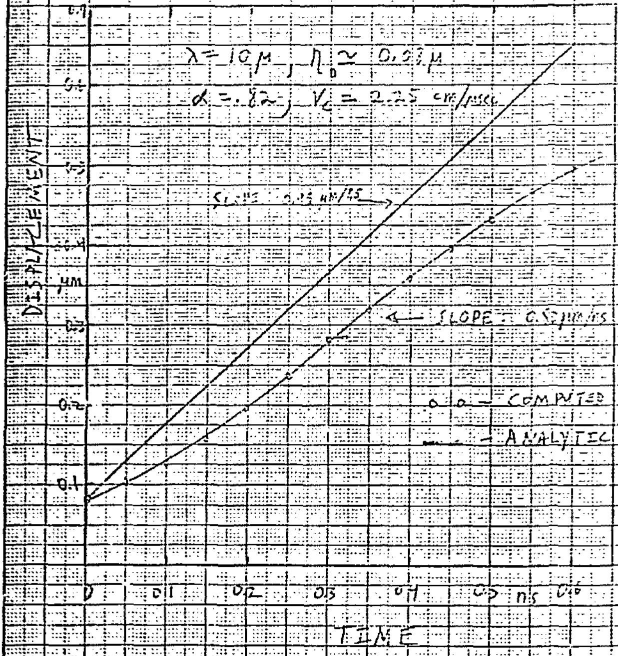
λ = 10 μ, η_D ≃ 0.03 μ
α = .82, V_c = 2.25 cm/μsec
SLOPE = 0.75 μm/ns
SLOPE = 0.55 μm/ns
o o — COMPUTED
— — ANALYTIC
DISPLACEMENT
μm
0.7
0.6
0.5
0.4
0.3
0.2
0.1
0
0.1
0.2
0.3
0.4
0.5
ns
0.6
TIME

FIGURE 9

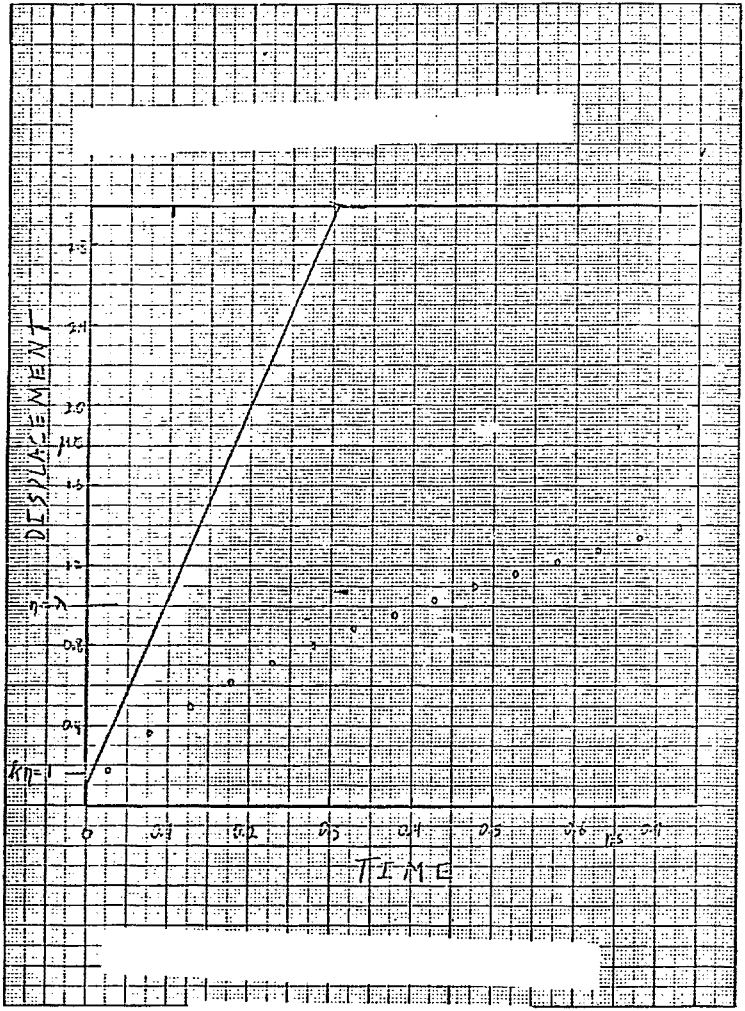
DISPLACEMENT
2.8
2.4
2.0
μc
1.6
1.2
η=λ
0.8
0.4
kη=1
0
0.1
0.2
0.3
0.4
0.5
0.6
1.5
0.7
TIME

FIGURE 10

INNER SURFACE INSTABILITY DURING DECELERATION

- Of potential importance for all ICF designs.
- Moderately short wavelengths ($\sim 10\ \mu$ and above) have non-negligible growth times.
- Very short wavelengths ($\lesssim 1\ \mu$) cause greatest concern.

FIGURE 11

INNER SURFACE INSTABILITY: POSSIBLE REMEDIES

- Obtain output before instability growth.
- Design targets with intermediate density layer for inner shell.
- Viscous and thermal diffusion.
- Mass diffusion.
- Turbulent mixing.

FIGURE 12